Available online at www.sciencedirect.com
ScienceDirect
Pattern Recognition 40 (2007) 825–838
PATTERN RECOGNITION
THE JOURNAL OF THE PATTERN RECOGNITION SOCIETY
www.elsevier.com/locate/pr

Fast and robust fuzzy *c*-means clustering algorithms incorporating local information for image segmentation

Weiling Cai, Songcan Chen*, Daoqiang Zhang

Department of Computer Science & Engineering, Nanjing University of Aeronautics & Astronautics, Nanjing 210016, PR China

Received 7 July 2005; received in revised form 12 June 2006; accepted 27 July 2006

Abstract

Fuzzy *c*-means (FCM) algorithms with spatial constraints (FCM_S) have been proven effective for image segmentation. However, they still have the following disadvantages: (1) although the introduction of local spatial information to the corresponding objective functions enhances their insensitiveness to noise to some extent, they still lack enough robustness to noise and outliers, especially in absence of prior knowledge of the noise; (2) in their objective functions, there exists a crucial parameter α used to balance between robustness to noise and effectiveness of preserving the details of the image, it is selected generally through experience; and (3) the time of segmenting an image is dependent on the image size, and hence the larger the size of the image, the more the segmentation time. In this paper, by incorporating local spatial and gray information together, a novel fast and robust FCM framework for image segmentation, i.e., fast generalized fuzzy *c*-means (FGFCM) clustering algorithms, is proposed. FGFCM can mitigate the disadvantages of FCM_S and at the same time enhances the clustering performance. Furthermore, FGFCM not only includes many existing algorithms, such as fast FCM and enhanced FCM as its special cases, but also can derive other new algorithms such as FGFCM_S1 and FGFCM_S2 proposed in the rest of this paper. The major characteristics of FGFCM are: (1) to use a new factor S_{ij} as a local (both spatial and gray) similarity measure aiming to guarantee both noise-immunity and detail-preserving for image, and meanwhile remove the empirically-adjusted parameter α; (2) fast clustering or segmenting image, the segmenting time is only dependent on the number of the gray-levels q rather than the size $N(\gg q)$ of the image, and consequently its computational complexity is reduced from $O(NcI_1)$ to $O(qcI_2)$, where c is the number of the clusters, I_1 and $I_2(< I_1,$ generally) are the numbers of iterations, respectively, in the standard FCM and our proposed fast segmentation method. The experiments on the synthetic and real-world images show that FGFCM algorithm is effective and efficient.

Keywords: Fuzzy *c*-means clustering (FCM); Enhanced fuzzy *c*-means clustering; Image segmentation; Robustness; Spatial constraints; Gray constraints; Fast clustering

1. Introduction

Image segmentation is widely used in a variety of applications such as robot vision, object recognition, geographical imaging and medical imaging [1–3]. Classically, image segmentation is defined as the partitioning of an image into non-overlapped, consistent regions which are homogeneous with respect to some characteristics such as gray value or texture. Fuzzy *c*-mean (FCM) [4] is one of the most used methods for image segmentation [5–8] and its success chiefly attributes to the introduction of fuzziness for the belongingness of each image pixels. Compared with crisp or hard segmentation methods [9], FCM is able to retain more information from the original image. However, one disadvantage of standard FCM is not to consider any spatial information in image context, which makes it very sensitive to noise and other imaging artifacts.

Recently, many researchers have incorporated local spatial information into the original FCM algorithm to improve the performance of image segmentation [9–12]. Tolias and Panas [11] developed a Sugeno-type rule-based system to enhance the results of fuzzy clustering by imposing spatial constraints. Pham [13] modified the FCM objective function

* Corresponding author. Tel.: +86 25 84896481x12106; fax: +86 25 84498069.
E-mail address: s.chen@nuaa.edu.cn (S. Chen).

0031-3203/$30.00
doi:10.1016/j.patcog.2006.07.011

by including a spatial penalty on the membership functions. The penalty term leads to an iterative algorithm, which is very similar to the original FCM and allows the estimation of spatially smooth membership functions. Ahmed et al. [14] modified the objective function of FCM to compensate for the gray (intensity) inhomogeneity and to allow the labeling of a pixel to be influenced by the labels in its immediate neighborhood, and they call the algorithm as FCM_S.

One disadvantage of FCM_S is that it computes the neighborhood term in each iteration step, which is very time-consuming. In order to reduce the computational loads of FCM_S, Chen and Zhang [15] proposed two variants, FCM_S1 and FCM_S2, which simplified the neighborhood term of the objective function of FCM_S. These two algorithms introduce the extra mean-filtered image and median-filtered image, respectively, which can be computed in advance, to replace the neighborhood term of FCM_S. Thus the execution times of both FCM_S1 and FCM_S2 are considerably reduced.

More recently, Szilágyi et al. [16] proposed enhanced fuzzy c-mean (EnFCM) algorithm to accelerate the image segmentation process. EnFCM is based on a simple fact about images, which is usually overlooked in many FCM-type algorithms. That is, the number of gray-levels q is generally much smaller than the size N of the image. By using this fact, the time complexity of EnFCM can be drastically reduced from $O(NcI_1)$ to $O(qcI_2)$. The structure of EnFCM is different from that of FCM_S and its variants. Firstly, a linearly-weighted sum image is formed from both original image and its local neighbor average gray image (refer to a definition later), and then clustering for the summed image is performed on the basis of the gray level histogram instead of pixels in the image. As a result, the computational load of EnFCM is much reduced. Besides, the quality of image segmented by EnFCM is comparable to that of FCM_S [16].

However, EnFCM still shares a common crucial parameter α with FCM_S and its two variants. The parameter α is used to control the tradeoff between the original image and its corresponding mean- or median-filtered image. The value of α has a crucial impact on the performance of those methods, but its selection is generally difficult because α should keep a balance between insensitiveness to noise and effectiveness of preserving the details. In other words, the value of α has to be chosen large enough to tolerate the noise, on the other hand, it also has to be chosen small enough to prevent the image from losing much of its sharpness and details [16]. From the above analysis for α, we can conclude that the determination of α is in fact noise-dependent in some degree. Because the types and intensity of the noise are generally a prior unknown, in practice, the selection of α is generally made by experience or by trial-and-error experiments [14–16]. Moreover, the value of α is fixed for all neighbor windows over the image and thus the local gray level or spatial information of the image may be overlooked.

In order to mitigate these defects of the selection of α and at the same time promote the image segmentation performance, in this paper, we propose the fast generalized fuzzy c-means (FGFCM) algorithms for fast and robust image segmentation. In FGFCM, a novel locality factor S_{ij} is defined to replace the parameter α in EnFCM and FCM_S and its variants. The new factor cannot only mitigate the defects of α but also possess several attractive characteristics as follows: (1) S_{ij} makes our algorithm relatively independent of the types of the noise, and thus in the absence of prior knowledge of the noise our algorithm is a better choice for segmentation; (2) S_{ij} incorporates simultaneously both the local spatial relationship and the local gray-level relationship and its value varies from pixel to pixel for the image, i.e., spatially and gray dependent; (3) S_{ij} can automatically be determined by local spatial and gray relationship rather than artificially or empirically selected like α, so the determination of the S_{ij} value is relatively easier than the value of α. All these characteristics make our algorithm more general and suitable for image clustering. From such a general framework, it is not difficult to find that it not only includes many existing algorithms such as fast versions of FCM and EnFCM [16] as its special cases, but also derives many other new algorithms such as FGFCM_S1 and FGFCM_S2 proposed in the rest of our paper. Furthermore, inspired by fast clustering or segmentation as in EnFCM, the segmenting time of the new derived clustering algorithms from the framework will be reduced from $O(NcI_1)$ to $O(qcI_2)$ compared with the standard FCM.

The rest of this paper is organized as follows. In Section 2, FCMs clustering algorithms with spatial constraints (FCM_S, FCM_S1 and FCM_S2) are introduced, followed by the EnFCM algorithm. In Section 3, we propose the FGFCMs algorithm including FGFCM, FGFCM_S1 and FGFCM_S2. The experimental comparisons are presented in Section 5. Finally, Section 4 gives our conclusions and several issues for future work.

2. Preliminaries

2.1. Fuzzy clustering with spatial constraints (FCM_S) and its variants

Ahmed et al. [14] proposed a modification to the standard FCM by introducing a term that allow the labeling of a pixel (voxel) to be influenced by labels in its immediate neighborhood [17]. The neighborhood effect acts as a regularizer and biases the solution toward piecewise-homogeneous labeling. The modified objective function of FCM_S is defined as follows:

$$J_m = \sum_{i=1}^{c}\sum_{k=1}^{N} u_{ik}^m \|x_k - v_i\|^2 + \frac{\alpha}{N_R}\sum_{i=1}^{c}\sum_{k=1}^{N} u_{ik}^m \sum_{r\in N_k} \|x_r - v_i\|^2, \quad (1)$$

where x_k is the gray value of the kth pixel, v_i represents the prototype value of the ith cluster, u_{ik} represents the fuzzy

membership of the kth pixel with respect to cluster i, N_R is its cardinality, x_r represents the neighbor of x_k and N_k stands for the set of neighbors falling into a window around x_k. The parameter m is a weighting exponent on each fuzzy membership that determines the amount of fuzziness of the resulting classification. The parameter α is used to control the effect of the neighbors term. By definition, each sample point x_k satisfies the constraint that $\sum_{i=1}^{c} u_{ik} = 1$. Two necessary but not sufficient conditions for J_m to be at its local extreme will be obtained as follows:

$$u_{ik} = \frac{\left(\|x_k - v_i\|^2 + \frac{\alpha}{N_R}\sum_{r\in N_k}\|x_r - v_i\|^2\right)^{-1/(m-1)}}{\sum_{j=1}^{c}\left(\|x_k - v_j\|^2 + \frac{\alpha}{N_R}\sum_{r\in N_k}\|x_r - v_j\|^2\right)^{-1/(m-1)}}, \tag{2}$$

$$v_i = \frac{\sum_{k=1}^{N} u_{ik}^m \left(x_k + \frac{\alpha}{N_R}\sum_{r\in N_k} x_r\right)}{(1+\alpha)\sum_{k=1}^{N} u_{ik}^m}. \tag{3}$$

The second term $\sum_{j\in N_k} x_j/N_R$ in the numerator of Eq. (3) is in fact a neighbor average gray value around x_k, the image composed of all the neighbor average values around all the image pixels forms a so-called local neighbor average image or equivalently mean-filtered image.

A shortcoming of Eqs. (2) and (3) is that computing the neighbor term will take much time in each iteration step. In order to reduce the computation, Chen and Zhang [15] proposed a variant of FCM_S, FCM_S1, which simplified the neighborhood term of FCM_S. And the low-complexity objective function can be written as follows:

$$J_m = \sum_{i=1}^{c}\sum_{k=1}^{N} u_{ik}^m \|x_k - v_i\|^2 + \alpha \sum_{i=1}^{c}\sum_{k=1}^{N} u_{ik}^m \|\overline{x_k} - v_i\|^2, \tag{4}$$

where $\overline{x_k}$ is a means of neighboring pixels lying within a window around x_k . Unlike Eq. (1), $\overline{x_k}$ can be computed in advance, thus, the clustering time can be saved when $\sum_{r\in N_k}\|x_r - v_i\|^2/N_R$ in Eq. (1) is replaced with $\|\overline{x_k} - v_i\|^2$. An iterative algorithm for minimizing Eq. (4) with respect to u_{ik} and v_i can similarly in FCM_S be derived, as shown in Eqs. (5)–(6):

$$u_{ik} = \frac{(\|x_k - v_i\|^2 + \alpha\|\overline{x_k} - v_i\|^2)^{-1/(m-1)}}{\sum_{j=1}^{c}(\|x_k - v_j\|^2 + \alpha\|\overline{x_k} - v_j\|^2)^{-1/(m-1)}}, \tag{5}$$

$$v_i = \frac{\sum_{k=1}^{N} u_{ik}^m (x_k + \alpha\overline{x_k})}{(1+\alpha)\sum_{k=1}^{N} u_{ik}^m}. \tag{6}$$

Therefore, Eqs. (2) and (3) obtain simplification to some extent. The essence of FCM_S1 is to make both the original image and the corresponding local neighbor (for example, 3×3) average or mean-filtered image have the same prototypes or segmentation result with aiming to guarantee the gray homogeneity. FCM_S1 not only considerably reduces the execution time for clustering an image but also improves the robustness to Gaussian noise [15].

However, FCM_S1 is unsuitable for the images corrupted by impulse noises such as salt and pepper noise [15]. In order to overcome that problem, the authors of Ref. [15] designed further FCM_S2, a variant of FCM_S1 in which the median-filtered image replaces the mean-filtered one, to enhance the robustness to impulse noises like salt and pepper noise, such an enhancement can be due to the incorporation of the local median-filtered image in clustering.

In both FCM_S1 and FCM_S2, there exists a crucial parameter α which controls the tradeoff between the original image and its corresponding mean- or median-filtered image. When α is set to zero, the algorithm is equivalent to the original FCM, while when it approaches infinite, the algorithm acquires the same effect as the original FCM on the mean- or median-filtered image, respectively.

FCM, FCM_S1 and FCM_S2 algorithms can be summarized as follows.

FCM_S, FCM_S1 and FCM_S2 Algorithms

Step 1: The number c of these prototypes or clusters ranges from 2 to $c_{\max}$, fix a certain value c and then select initial class prototypes and set $\varepsilon > 0$ to a very small value.

Step 2: For FCM_S1 and FCM_S2 only, compute the mean or median filtered image.

Step 3: Update the partition matrix using Eq. (2) (FCM_S) or Eq. (5) (FCM_S1 and FCM_S2).

Step 4: Update the prototypes using Eq. (3) (FCM_S) or Eq. (6) (FCM_S1 and FCM_S2).

Repeat Steps 3 and 4 until the following termination criterion is satisfied:

$$|V_{new} - V_{old}| < \varepsilon,$$

where $V = [v_1, v_2, \ldots, v_c]$ are the vectors of cluster prototypes.

2.2. Enhanced fuzzy c-means

Szilágyi et al. [16] proposed the EnFCM algorithm to speed up the segmentation process for gray-level image. In order to accelerate FCM_S, a linearly-weighted sum image ξ is in advance formed from the original image and its local neighbor average image in terms of

$$\xi_k = \frac{1}{1+\alpha}\left(x_k + \frac{\alpha}{N_R}\sum_{j\in N_k} x_j\right), \tag{7}$$

where ξ_k denote the gray value of the kth pixel of the image ξ, x_j represents the neighbors of x_k, N_k stands for the set of neighbors falling into a window around x_k and $\sum_{j\in N_k} x_j/N_R$ plays again the same role as mean-filtered pixel value as in Eq. (3). The α plays the same role as before. Then, the fast segmentation method [16] is performed

on the gray-level histogram of the generated image ξ. Concretely, the objective function used for fast segmenting the newly-generated image ξ is defined as

$$J_s = \sum_{i=1}^{c}\sum_{l=1}^{q} \gamma_l u_{il}^m (\xi_l - v_i)^2, \tag{8}$$

where v_i represents the prototype of the ith cluster, u_{il} represents the fuzzy membership of gray value l with respect to cluster i. q denotes the number of the gray levels of the given image which is generally much smaller than N. γ_l is the number of the pixels having the gray value equal to l, where $l = 1, \ldots, q$. Naturally, we have

$$\sum_{l=1}^{q} \gamma_l = N. \tag{9}$$

And under the constraints that $\sum_{i=1}^{c} u_{il} = 1$ for any l, minimize J_s. Specifically, taking the first derivatives of J_s with respect to u_{il} and v_i, and zeroing them, respectively, two necessary but not sufficient conditions for J_s to be at its local extrema will be obtained as follows:

$$u_{il} = \frac{(\xi_l - v_i)^{-2/m-1}}{\sum_{j=1}^{c} (\xi_l - v_j)^{-2/m-1}}, \tag{10}$$

$$v_i = \frac{\sum_{l=1}^{q} \gamma_l u_{il}^m \xi_l}{\sum_{l=1}^{q} \gamma_l u_{il}^m}. \tag{11}$$

Now, EnFCM Algorithm is summarized as follows:

EnFCM Algorithm

Step 1: The number c of these prototypes or clusters ranges from 2 to $c_{\max}$, fix a certain value c and then select initial class prototypes and set $\varepsilon > 0$ to a very small value.

Step 2: Compute the new image ξ in terms of Eq. (7) in advance.

Step 3: Update the partition matrix using Eq. (10).

Step 4: Update the prototypes using Eq. (11).

Repeat Steps 3 and 4 until the following termination criterion is satisfied:

$$|V_{new} - V_{old}| < \varepsilon,$$

where $V = [v_1, v_2, \ldots, v_c]$ are the vectors of cluster prototypes.

The significant reduction of execution time attributes to taking the range or distribution of gray levels of given image into account, which is usually overlooked in many FCM-type algorithms including FCM, FCM_S, FCM_S1 and FCM_S2 etc. Due to that the gray value of the pixels is generally encoded with 8-bit resolution, equivalently, 256 levels in total, and thus the number q of gray levels is generally much smaller than the size N of the image. Consequently, the time complexity is drastically reduced from $O(NcI_1)$ to $O(qcI_2)$ especially for the large image.

EnFCM provides comparable segmenting quality in considerably fast manner for the brain image used there [16] to FCM_S, but the segmenting quality depends on the chosen window size, the parameter α and the filtering method. The value of α has to be chosen large enough so that it can eliminate noise, on the other hand, it also has to be chosen small enough so that the after-segmented image does not lose much of its sharpness and details. However, because of having no prior knowledge about the noise, its selection is not so easy. In addition, in order to make a balance between noise-immunity and detail-preserving with no prior knowledge, we have to select it by experience or the trial-and-error method.

3. Fast generalized fuzzy c-means algorithms

FCM_S1 and FCM_S2, as two extensions to FCM_S, have yielded effective segmentation for images [15], but both still have some disadvantages: (1) although the introduction of local spatial information enhances their insensitiveness to noise to some extent, FCM_S1 and FCM_S2 still lack enough robustness [18–21] to noise and outliers, especially in absence of prior knowledge of the noise; (2) in their objective functions, there exists a crucial parameter α used to balance between robustness to noise and effectiveness of preserving the details of the image, and generally its selection has to be made by experience; and (3) the time of segmenting an image is heavily dependent on the image size, the larger the size, the more the time-consuming.

EnFCM speeds up the FCM_S and significantly reduces the execution time by clustering on gray-level histogram rather than on pixels, however, it also lacks enough robustness to noise, especially mixed noises and has to select empirically the trade-off parameter α in the FCM_S type algorithms.

Motivated by individual strengths of FCM_S1, FCM_S2 and EnFCM, we propose a novel fast and robust FCM framework for image segmentation in this paper called FGFCM clustering algorithms incorporating local information.

3.1. A novel local (spatial and gray) similarity measure S_{ij}

FCM_S, FCM_S1, FCM_S2 and EnFCM all share a common parameter α and its selection is generally important as well as difficult. The importance is due to that the parameter α must be adopted to make some balance between robustness to noise and effectiveness of preserving the details for image. And the difficulty of its selection results from such a fact that the determination of α is noise-dependent but the types and intensity of the noise are generally a priori unknown and thus extensive trial-and-error experiments has to be carried out, which significantly increases the computational burden. Even if the prior knowledge of noise can be known, the adjustment for it also should follow such a rule of thumb [14] that its value must be taken large enough for

those pixels corrupted by relatively heavy noise, which will unavoidably incur unnecessary blur for pixels not corrupted by the noise and thus lead to loss of some details in image. On the other hand, its value should be small for those pixels with no and little noise corruption. Therefore, setting the same value of α for all the neighbors of the pixels over the image during segmentation or clustering is intuitively obviously unreasonable. In other words, the setting for α should take into account: (1) the spatial or location relationship of pixels within the neighbor window, for example, when the window size is expanded from 3×3 to 5×5, α should be set to different value for different spatial distance from the center of the window, otherwise some blur is unavoidably introduced for given image; (2) the gray level or intensity relationship of the pixels within the same window, such a relationship can reflect the local neighborhood inhomogeneity of the window and thus setting the different values of α for different pixels within the window cannot only suppress the influence of the outlier but also avoid blur for given image to some extent.

To remedy the above two shortcomings of adopting a common α, we introduce a novel factor S_{ij} incorporating both the local spatial relationship (called S_{s_ij}) and the local gray-level relationship (called S_{g_ij}) to replace the parameter α and make it play a more important role in clustering. Its definition is presented as below:

$$S_{ij} = \begin{cases} S_{s\_ij} \times S_{g\_ij}, & j \neq i, \\ 0, & j = i, \end{cases} \tag{12}$$

where the ith pixel is the center of the local window (for example, 3×3) and jth pixel are the set of the neighbors falling into a window around the ith pixel.

It is easy to see that the introduction of S_{s_ij} naturally overcomes the first limitation of using a common α over an image in FCM_S etc. S_{s_ij} makes the influence of the pixels within the local window change flexibly according to their distance from the central pixel and thus more local information can be used. Here the definition of S_{s_ij} is given as follows:

$$S_{s\_ij} = \exp\left(\frac{-\max(|p_j - p_i|, |q_j - q_i|)}{\lambda_s}\right), \tag{13}$$

where (p_i, q_i) is a spatial coordinate of the ith pixel and we assume one pixel is one unit length in the above computation. λ_s denotes the scale factor of the spread of S_{s_ij}, determining the change characteristic of S_{s_ij}, thus its varying range is relatively easily determined. It is worth indicating that the shape of local window defined here is square, however, the windows with other shapes such as diamond can also naturally be adopted in our algorithm. As a whole, S_{s_ij} reflects the damping extent of the neighbors with the spatial distances from the central pixel. In contrast, the parameter α in FCM_S, FCM_S1, FCM_S2 and EnFCM is globally taken as a constant and thus it is relatively difficult to vary adaptively with different spatial locations or distances from the central pixel. When λ_s are set to 1, 3 and 10, respectively,

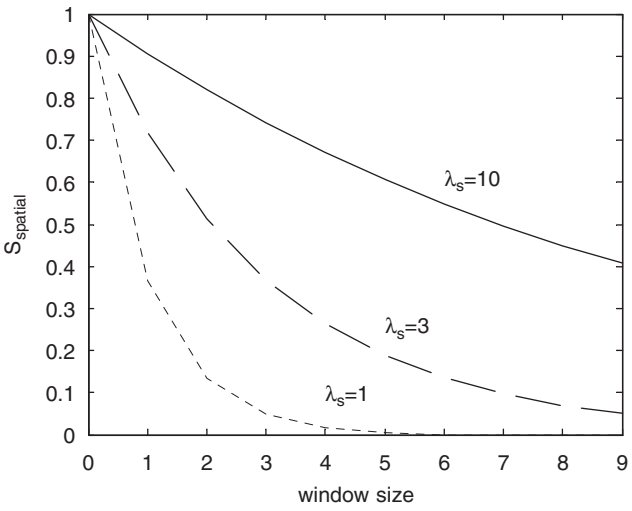

Fig. 1. Changing trend of S_{s_ij} against the size of the window.

the changing trend of S_{s_ij} against the size of the window are shown as below:

From Fig. 1, we can see that for some λ_s, the nearer to the window center the location is, the larger the S_{s_ij} value is, thus S_{s_ij} reflects different damping extent for pixels according to different spatial locations within a given window.

In order to mitigate the second shortcoming resulting from the same parameter α, we define the local gray-level similarity measure S_{g_ij} as follows:

$$S_{g\_ij} = \exp\left(\frac{-\|x_i - x_j\|^2}{\lambda_g \times \sigma_{g\_i}^2}\right), \tag{14}$$

where σ_{g_i} is defined by

$$\sigma_{g\_i} = \sqrt{\frac{\sum_{j \in N_i} \|x_j - x_i\|^2}{N_R}}, \tag{15}$$

where x_i is gray value of the central pixel within a special window, x_j is gray value of the jth pixels in the same window, and λ_g denotes the global scale factor of the spread of S_{g_ij} and plays a similar role to λ_s. The parameter σ_{g_i} is a function of the local density surrounding the central pixel and its value reflects gray value homogeneity degree of the local window. The smaller its value is, the more homogenous the local window is, and vice versa. The motivation behind the use of pixel-dependent parameter σ_{g_i} is to exploit the local statistics varying with each image pixel. The autodetermined parameter σ_{g_i} can be computed in advance according to Eq. (15) and its value is different from pixel to pixel of a given image. By the definition of S_{g_ij}, we know that when the gray value of the jth neighbors of x_i is close to the gray value of x_i, S_{g_ij} should be large and vice versa. Obviously, the S_{g_ij}s can change automatically with different gray levels of the pixels over an image and thus reflects the damping extent in gray values.

Although there are two parameters in the proposed method, in practice only one parameter λ_g need to be adjusted. The reason is that another parameter λ_s can be determined in advance once the size of windows is specified. In this paper, we fix the parameter λ_s to 3 in all experiments. Therefore, only a global parameter λ_g need to be adjusted. Moreover, due to its geometrical implication, the selection of λ_g is relatively much easier than that of the parameter α in other methods such as FCM_S and its variants. In our experiments, λ_g is selected from 0.5 to 6 with the increment 0.5, while the parameter α is selected from 0.2 to 8 with the increment 0.2. Thus, the choice of λ_g is easier than that of α.

3.2. General framework of FGFCM

By introducing the definition of S_{ij} and combining the idea from FCM_S1, FCM_S2 and EnFCM, we propose a novel fast and robust FCM framework for image segmentation: FGFCM clustering algorithms. It incorporates local spatial and gray-level information into its objective function. Further by taking the place of a constant parameter α in Eq. (7) with S_{ij} varying from pixel to pixel within the local window, the new generated image ξ is computed in terms of:

$$\xi_i = \frac{\sum_{j\in N_i} S_{ij} x_j}{\sum_{j\in N_i} S_{ij}}, \tag{16}$$

where ξ_i denotes the gray value of the ith pixel of the image ξ, x_j represents gray value of the neighbors of x_i (window center), N_i is the set of neighbors falling in the local window and S_{ij} is the local similarity measure between the ith pixel and the jth pixel. The value of ξ_i is restricted to [0, 255] due to the denominator. In Eq. (16), S_{ij} can be considered as the weight of the jth pixel and ξ_i can be considered as the ith pixel of the linearly-weighted summed image.

Replacing Eq. (7) with Eq. (16), we can get FGFCM algorithm as below:

FGFCM Algorithm

Step 1: (1) Set the number c of the cluster prototypes change from 2 to $c_{\max}$ (predefined or set by some validity criterion or a priori knowledge).

(2) Initialize randomly those prototypes and set $\varepsilon > 0$ to a very small value.

Step 2: Compute the local similarity measures S_{ij} using Eq. (12) for all neighbor windows over the image.

Step 3: Compute linearly-weighted summed image ξ in terms of Eq. (16).

Step 4: Update the partition matrix using Eq. (10).

Step 5: Update the prototypes using Eq. (11).

Repeat Steps 4 and 5 until the following termination criterion is satisfied:

$$|V_{new} - V_{old}| < \varepsilon,$$

100	25	25	→	0.0499	0.9848	0.9848
28	30	30		0.9976	0	1.0000
30	120	35		1.0000	0.0071	0.9848

Fig. 2. 3×3 window with noise and the corresponding value of S_{ij}.

where $V = [v_1, v_2, \ldots, v_c]$ are the vectors of cluster prototypes.

The optimization flowcharts used in this algorithm is called a fixed-point iteration (FPI) or alternate optimization (AO) as in FCM, the iteration process will terminate at the user-specified number of iteration or local minima of the corresponding objective functions. Consequently, optimal or locally optimal results can always be ensured.

The measure used in the FGFCM objective function is still the Euclidean metric as in FCM, which is computationally simple. Moreover, different from FCM, FGFCM is robust because of the introduction of the factor S_{ij}, which can be analyzed as follows:

Seen from Eq. (16), the noise tolerance and outliers resistance property of ξ_i completely relies on the definition of S_{ij}. In the absence of prior knowledge of the noise, S_{ij} should automatically be determined rather than artificially set. Especially, the S_{ij} of the noise-corrupted pixels within a window should keep small and thus the influence of noise can be ignored. The S_{ij} used in FGFCM can be adaptively changed and thus guarantee the insensitive to noise and outliers. The presence of the noise and outliers can generally be divided into two cases below:

(1) The central pixel is not a noise and some pixels within its local window may be corrupted by noise. In this situation, the gray values of the noisy pixels are far different from the other pixels within the window, and thus the S_{g_ij}s of these corrupted pixels and the corresponding S_{ij}s are small due to the function characteristics in Eqs. (12)–(14). Therefore, the weighted sum of image pixel shall be suppressed and hence more robust to outliers. The following example of Fig. 2 clearly illustrates this situation in which the entries of the 3×3 window on the right hand side can be computed in terms of Eq. (12). For example, the corresponding value of S_{ij} of the first pixel with gray value 100 is 0.0499 in the right window.

(2) The central pixel is a noise and the other pixels within its local window are homogenous, i.e., having small σ_{g_i}. In this situation, the S_{ij}s of these pixels within the local window (excluding x_i) have almost same values and the S_{ij} of the central pixel equals zero. Therefore, ξ_i is hardly influenced by the central pixel. Such situation is clearly demonstrated by Fig. 3.

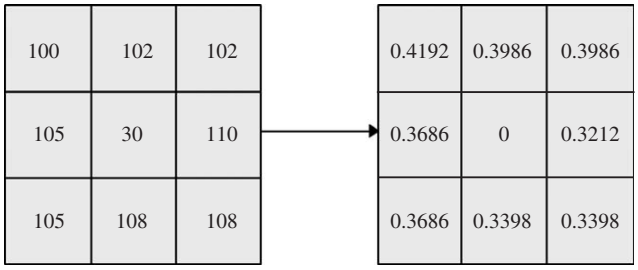

Fig. 3. 3×3 window with noise and the corresponding value of S_{ij}.

The above two examples just give some intuitive illustrations about the robustness of our algorithm. In fact, their theoretical ground can also be verified from the viewpoint of robustified filters [22,23] and locality-based methods [24]. Concretely, according to the robust filtering viewpoint, the reformulation of Eq. (16) is similar to the filtered result derived by optimizing a kernel-induced robust measure [25,26] based on classical linear mean filter. On the other hand according to the locality-based methods, the incorporation of the S_{ij} with spatial and gray localities to Eq. (16) can also enhance its robustness to noise and outliers. Due to the space limit, we omitted the details of the proof here.

It is also worth to point out that the denoising method used in FGFCM is different from the one used in FCM_S1 and FCM_S2. FCM_S1 is relatively suitable for the noisy image corrupted by Gaussian noise due to using a mean-type filtering, while FCM_S2 is relatively suitable for the image corrupted by impulse noises like salt and pepper noise due to use of a median-type filtering. And the final effectiveness of removing the noise in clustering relies on the value of the parameter α. Without the prior knowledge of the noise, it is generally hard to choose the proper one between FCM_S1 and FCM_S2 and the optimal value of α for image segmentation. Compared with FCM_S1 or _S2, the denoising method in FGFCM is independent of the type of noise and its effectiveness seems insensitive to the spatial scale factor λ_s and the gray-level scale factor λ_g to some extent as shown in the experiments later.

S_{ij} not only guarantees the robustness to noise and outliers but also seems to preserve more image information. It incorporates both local spatial relationship S_{s_ij} which changes adaptively according to spatial distances from the central pixel, and the local gray-level relationship S_{g_ij} which varies automatically according to different gray-level difference between the pixels over an image. Thus, the value of S_{ij} varies from pixel to pixel within a neighbor window, which likely preserves more information than using same value for each pixel. Therefore, FGFCM adopting S_{ij} seems able to perserve more image details than EnFCM.

In the following, major characteristics of FGFCM are summarized:

(1) Using a new factor S_{ij} as a local (spatial and gray) similarity measure with aiming to guarantee both noise-immunity and detail-preserving for image, and at the same time remove the empirically-adjusted parameter α.
(2) Fast clustering or segmentation for given image, the segmenting time is only dependent on the number of the gray-levels q rather than the size N ($\gg q$) of the image, and consequently its computational complexity is reduced from $O(NcI_1)$ to $O(qcI_2)$.

3.3. Relationship between FGFCM and other methods

FGFCM clustering algorithms can be considered as a general framework. In fact, the structure of the framework FGFCM can be decomposed into the following two steps. In the first step, a linearly-weighted sum image ξ is generated according to different definition of S_{ij}, and in the second step, the fast segmentation method [16] is performed on the gray-level histogram of the generated image ξ.

Besides FGFCM, some other typical clustering algorithms for image segmentation can be derived from the framework according to different definition of S_{ij} as follows:

(1) By directly setting S_{ij} in Eq. (16) in terms of

$$S_{ij} = \begin{cases} 1, & j = i, \\ 0, & j \neq i, \end{cases} \tag{17}$$

FGFCM algorithm reduces into fast versions of the standard FCM, which is a special case of FGFCM.

(2) By directly setting S_{ij} in Eq. (16) in terms of

$$S_{ij} = \begin{cases} \dfrac{\alpha}{N_R}, & j \neq i, \\ 1, & j = i, \end{cases} \tag{18}$$

FGFCM algorithm reduces into EnFCM, that is, the latter is a special case of FGFCM algorithm.

(3) Motivated by FCM_S1, S_{ij} in Eq. (16) is defined as

$$S_{ij} = 1 \quad \text{for all } i \text{ and } j, \tag{19}$$

and naturally ξ_i equals to the mean of the neighbors within a specified window including the ith pixel. And this algorithm derived from FGFCM framework is called FGFCM_S1.

(4) Motivated by FCM_S2, S_{ij} in Eq. (16) is defined as

$$S_{ij} = \begin{cases} 1, & j = j^*, \quad j^* = \underset{j}{\text{median}}(x_j), \\ 0, & j \neq j^*, \end{cases} \tag{20}$$

and consequently ζ_i equals to the median of the neighbors within a specified window including the ith pixel. And this algorithm is named FGFCM_S2 under the framework of FGFCM.

4. Experiment results

In this section, we compare the effectiveness and efficiency of six algorithms FCM_S1, FCM_S2, EnFCM,

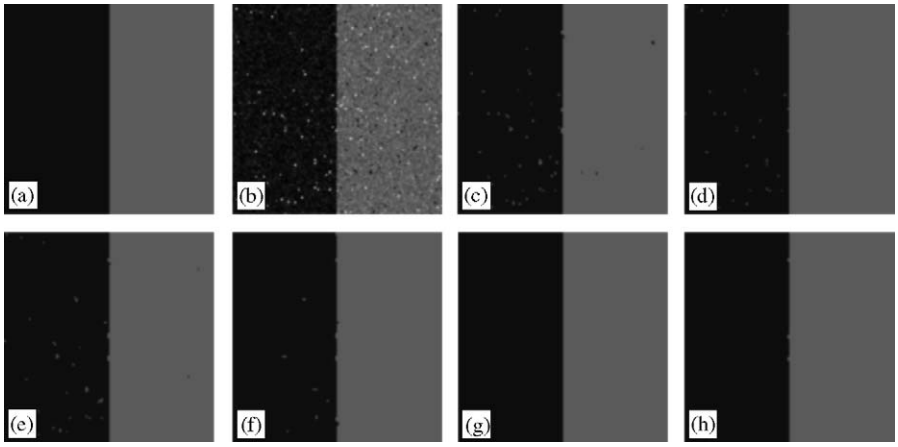

Fig. 4. Segmentation results on synthetic test image: (a) original image, (b) the same image with mixed noise, (c) FCM_S1 result, (d) FCM_S2 result, (e) EnFCM result, (f) FGFCM_S1 result, (g) FGFCM_S2 result, and (h) FGFCM result.

FGFCM_S1, FGFCM_S2 and FGFCM on some synthetic and real images. In all the following experiments, we set the parameters $\lambda_s = 3$, $\varepsilon = 0.00001$ and $N_R = 8$ (a 3×3 window centered around each pixel, except the central pixel itself).

In our experiments, we use the images corrupted, respectively, by the Gaussian noise and salt and pepper noise to test the robustness of the algorithms. Besides the above two types of noises, we also use the images with the mixed noise for more practical applications, this mixed noise is not simply pure Gaussian or impulsive noise but mixture of both whose distribution obeys $P_\eta = (1-\eta)G + \eta S$ where G denotes the Gaussian with zero mean and variance of σ_G^2 and S the $S\alpha S$ (symmetric α-stable, here abuse parameter α) with location θ and dispersion γ_s and thus the characteristic function $\varphi(t)$ [27,28] of P_η can be formulated as

$$\varphi(t) = \exp\left(j\eta\theta t - (1-\eta)^2 \frac{\sigma_G^2}{2} t^2 - \eta^\alpha \gamma_S |t|^\alpha \right), \quad \eta \in [0, 1], \tag{21}$$

where the parameter α controls how impulsive the distribution is. The η used in the following experiment is set to $2/(2 + (\pi)$ [28].

4.1. Results on synthetic image

To compare the denoising performances of the above six algorithms, we apply these algorithms to a synthetic test image as shown in Fig. 4(a) (128×128 pixels, two classes with two gray values taken as 0 and 90) corrupted by different levels of Gaussian noise, salt and pepper noise and mixed noise, respectively. The mixed noise used in this experiment is the mixture of Gaussian white noise N (0,100) and unit dispersion, zero centered symmetric α-stable ($S\alpha S$) noise. The parameters used in each noisy image are $c = 2$ and $\lambda_g = 6$. And at the same time, αs in the algorithms of FCM_S1, FCM_S2 and EnFCM are all chosen as 3.8 [15] which is obtained by searching the interval [0.2, 8] with respect to the optimal segmentation accuracy (SA), where SA is defined as the sum of the total number of pixels divided by the sum of number of correctly classified pixels [14].

4.1.1. Comparison of segmentation results on synthetic image corrupted by mixed noise

Fig. 4 are the segmenting results on a corrupted image with mixed noise ($\alpha = 0.7$ in $S\alpha S$). FCM_S1, _S2 and EnFCM are, respectively, affected by the noise to different extents which indicates that these algorithms lack enough robustness to the mixed noise. Visually, FGFCM_S1 removes most of the noise, FGFCM_S2 and FGFCM algorithms achieve relatively satisfactory results. More detailed quantified comparisons according to SA on different noise levels are given in the next subsection.

4.1.2. SA of the six algorithms on different noisy synthetic images

Table 1 gives the SAs of the six algorithms on the synthetic images corrupted, respectively, by different noises with different levels. From Table 1, we can see that the newly-proposed FGFCM-type algorithms give rise to better denoising performance than both FCM_S type and EnFCM algorithms, where FGFCM_S1 and FGFCM are the best and the second best in the presence of different Gaussian noise levels from 3% to 8%, while FGFCM_S2 and FGFCM display the best and second best performance in the presence of salt and pepper and mixed noise, respectively, with different levels, thus have better robustness to both impulse-type and mixed noises than all the other four algorithms. This analysis also indicates that FGFCM can relatively achieve a trade-off among Gaussian, impulse and mixed noises. Similarly, from the same table, we can observe that according to the SA, although EnFCM is inferior or comparable to FGFCM_S1 and FGFCM, respectively, under different Gaussian noise

Table 1
SA % of six algorithms on synthetic image

	FCM_S1	FCM_S2	EnFCM	FGFCM_S1	FGFCM_S2	FGFCM
Gaussian 3%	99.14	98.78	99.50	**99.57**	99.13	**99.51**
Gaussian 5%	96.42	96.12	97.65	**98.20**	96.82	**98.10**
Gaussian 8%	92.32	92.23	94.62	**95.41**	93.12	**95.10**
pepper&salt 5%	98.69	98.77	98.05	99.07	**99.99**	**99.91**
pepper&salt 10%	97.14	97.54	94.77	96.47	**99.98**	**99.47**
pepper&salt 15%	94.78	95.98	94.94	92.40	**99.84**	**98.36**
mixed noise $\alpha = 0.3$	93.80	97.25	95.34	95.82	**99.65**	**97.75**
mixed noise $\alpha = 0.5$	98.68	99.27	99.09	99.44	**99.97**	**99.84**
mixed noise $\alpha = 0.7$	99.59	99.79	99.69	99.83	**100.00**	**99.96**

corruptions, it is superior to two FCM_S type counterparts under the same corruption. However, this case is not always held for both impulse and mixed noises, now FCM_S2 is superior to EnFCM. In sum, FGFCM can be relatively suitable for segmenting images corrupted by unknown noise and achieve comparable performance (no matter what type of the noise is) to FGFCM_S1 in presence of Gaussian noise or to FGFCM_S2 in the presence of salt and pepper and mixed noise, respectively, in other words, its robustness seems basically independent of the noise type, which may attribute to the introduction of S_{ij}. On the whole, if the type of the noise is known, FGFCM_S1 is a better choice for the Gaussian noise, and FGFCM_S2 is a superior option for the salt and pepper noise; if the type of the noise is unknown, FGFCM seems to be a preferable selection.

4.1.3. Parameter analyses and selection in FGFCM, FCM_S1, FCM_S2 and EnFCM

In fact, those algorithms have some crucial parameters required to be adjusted for clustering and the parameters (λ_g in FGFCM and α in FCM_S1, _S2 and EnFCM) are noise-dependent, so their selection will obviously influence the segmenting result. In this section, we focus on discussion on the parameter selection on the synthetic image Fig. 4(a) corrupted by three types of noises.

Fig. 5 show the numbers of misclassified pixels of FGFCM, FCM_S1, _S2 and EnFCM varying with the parameters on the synthetic image Fig. 4(a) corrupted by three types of noises, respectively. From Fig. 5(a), we can see that the changing trend of misclassification of FGFCM against λ_g assumes monotonous decrease and relative smoothness after $\lambda_g = 3$ on the three types of noises, respectively. Alternately, it can be seen from Fig. 5(b)–(d) that, in the presence of Gaussian noise and mixed noise, the varying trends of FCM_S1, _S2 and EnFCM are, respectively, monotonously decreasing and then tend to be stable as α increases, respectively. However, the changing trends of three algorithms in the presence of salt and pepper noise are all unstable. On the whole, FGFCM is relatively insensitive to the λ_g to some extent and thus its choice for λ_g in FGFCM is easier than for α in FCM_S1, _S2 and EnFCM.

4.2. Results on real images corrupted by noises

In the following experiments, we first execute the six segmentation algorithms on a real image *eight* contaminated by mixed noise to investigate the robustness of the algorithms in Section 4.2.1. Then, we utilize the relatively large local window on a real *brain MR* image to inspect the influence of the window size on the algorithms' effectiveness in Section 4.2.2. Finally, the Section 4.2.3 gives the corresponding quantitative comparisons for the segmenting results presented in Sections 4.2.1 and 4.2.2.

4.2.1. Results on eight corrupted by mixed noise with 3×3 local window

To examine the algorithms' robustness, we apply the six algorithms on a real image *eight* [29] corrupted by mixed noise. Fig. 6(a) is the original image (308×242 pixels) with no noise and Fig. 6(b) is the same image corrupted simultaneously by Gaussian white noise N (0,180) and unit dispersion, zero centered symmetric α (α=0.9)-stable ($S\alpha S$) noise.

The segmenting results on Fig. 6(b) are shown in Figs. 6(c)–(h) and the parameters are $c = 3$, $\alpha = 8$ and $\lambda_g = 2$. From Figs. 6(c)–(h), we can visually see that FCM_S1, _S2, EnFCM and FGFCM_S1 are all influenced by the noise to different extents, respectively, which indicates that these algorithms lack enough robustness to the mixed noise, while FGFCM_S2 and FGFCM can basically eliminate the effect of the mixed noise. It can be concluded from the results of both FGFCM_S2 and FGFCM that although the denoising method in these two algorithms are quite different, these two approaches are both comparatively suitable for the images with mixed noise to some extent.

Here it is worth noting that with the special selection of α, EnFCM can become FGFCM_S1 as represented in Eqs. (18) and (19) and thus producing almost the same segmentation.

Besides, we also perform the same six algorithms on *eight* corrupted, respectively, by Gaussian noise and salt and pepper noise. From these results, it can be summarized that the relationship between the noise type and the six algorithms is almost identical to the conclusion drawn from the

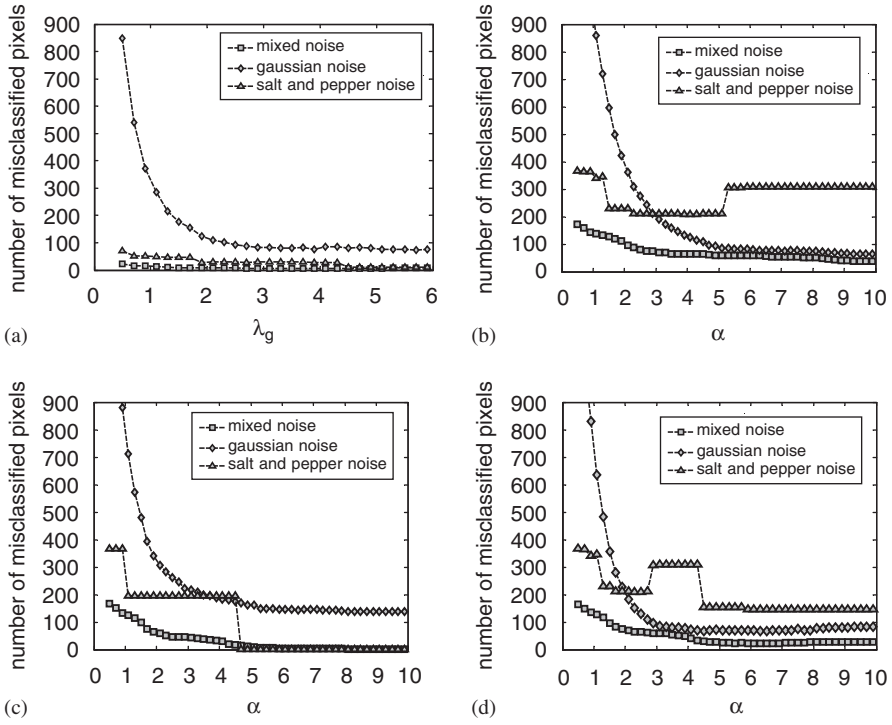

Fig. 5. Classification errors against the parameters on the synthetic image corrupted by Gaussian, salt and pepper and mixed noise, respectively: (a) FGFCM, (b) FCM_S1, (c) FCM_S2, and (d) EnFCM.

experimental result on the synthetic image in Section 4.1 and also consistent with the theoretical analysis about FGFCM in Section 3.2.

4.2.2. Results on brain MR image corrupted by mixed noise with 5×5 local window

In order to further examine the algorithms' effectiveness under a condition of the relatively large local window, we apply the same six algorithms on Fig. 7(b) with the local window of the size 5×5 rather than the ordinary size 3×3. Fig. 7(a) is a real *brain MR* slice (256×256 pixels) with no noise and Fig. 7(b) shows the same image corrupted simultaneously by Gaussian white noise N (0,180) and unit dispersion, zero centered symmetric α-stable ($S\alpha S$ $\alpha = 0.9$) noise.

Figs. 7(c)–(h) display the corresponding segmenting results of the six algorithms and here the parameters are $c = 3$, $\lambda_g = 0.5$, $\alpha = 5$ and $N_R = 24$. From Figs. 7(c)–(h), we can observe that when the window size is expanded to 5×5, the images segmented by FCM_S1, _S2, EnFCM, FGFCM_S1 and _S2 are heavily blurred to different extents, while such a blurred effect is not visually so obvious for FGFCM. As shown in Fig. 7(h), FGFCM preserves enough details from the corrupted image especially in the area marked by the ellipse. Therefore, FGFCM is a preferable choice in the situation where the clustering needs to use more spatial information or larger local window while no prior information related to noise is given.

4.2.3. Quantitative segmenting results comparisons

Furthermore, we also tabulate a quantitative segmenting comparison in Table 2 of these algorithms for Figs. 6(c)–(h) and 7(c)–(h) by calculating their scores defined by the following quantitative index [30,31]:

$$r_{ij} = \frac{A_{ij} \cap A_{refj}}{A_{ij} \cup A_{refj}}, \tag{22}$$

where A_{ij} represents the set of pixels belonging to the jth class found by the ith algorithm and A_{refj} represents the set of pixels belonging to the jth class in the reference segmented image. r_{ij} is in fact a fuzzy similarity measure, indicating the degree of equality between A_{ij} and A_{refj}, and the larger the r_{ij}, the better the segmentation is. From Figs. 6 and 7 and Table 2, FGFCM outperforms consistently the other five algorithms, respectively, which can again attribute to the introduction of the factor S_{ij} guaranteeing both relative insensitive to noise and outliers and detail-preserving.

4.3. Comparisons of segmentation time

In the Section 3, we have theoretically analyzed the computational complexity of the second step in the FGFCM framework and the goal of this subsection is to further experimentally investigate its practical acceleration for image segmentation relative to standard FCM (FCM for short). Here we apply the fast segmentation and FCM method on the after-filtered images $\xi - 1$, $\xi - 2$, $\xi - 3$ and $\xi - 4$.

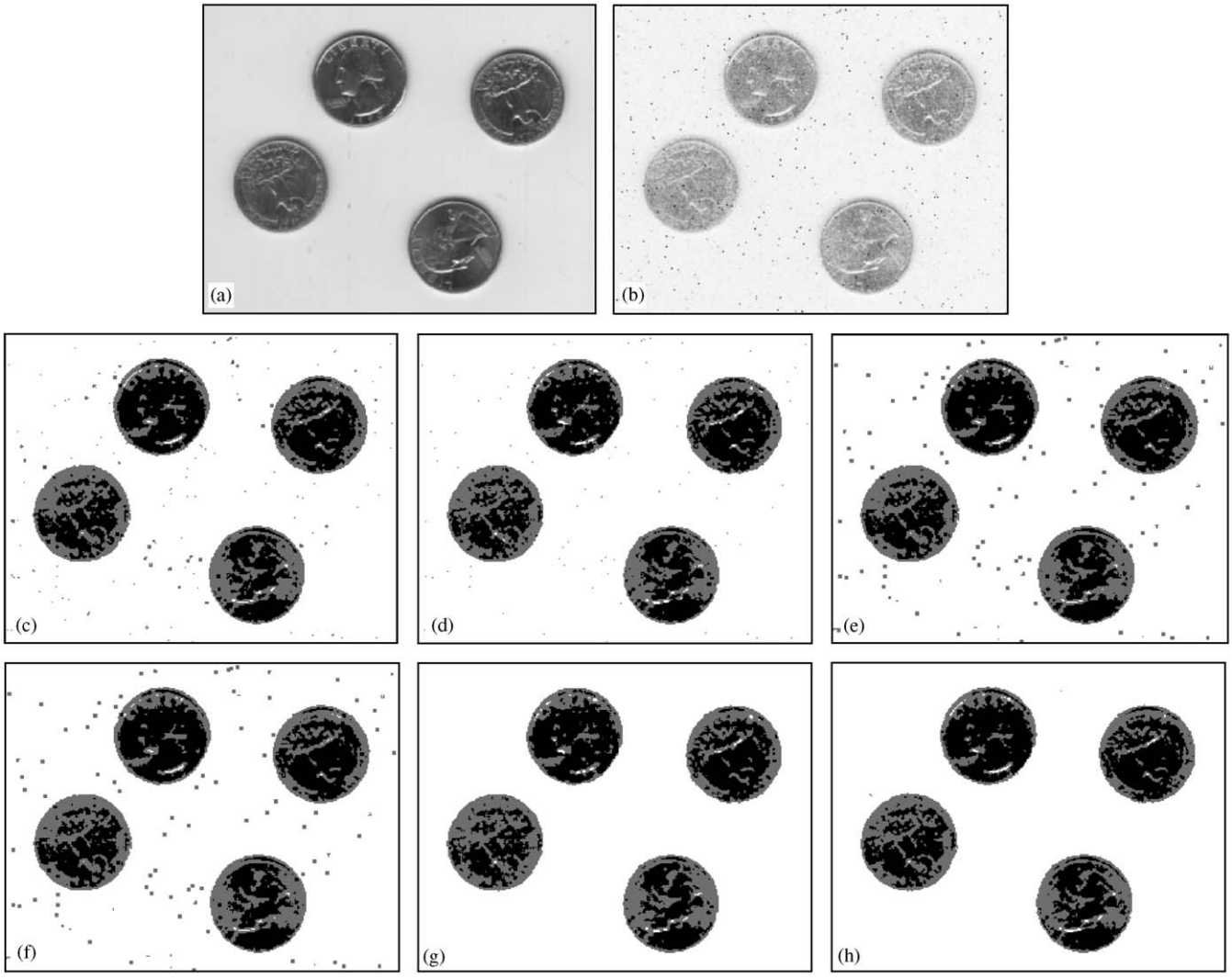

Fig. 6. Segmentation results on *eight* with mixed noise: (a) original image, (b) noisy image, (c) using FCM_S1, (d) using FCM_S2, (e) using EnFCM, (f) using FGFCM_S1, (g) using FGFCM_S2, and (h) using FGFCM.

Table 2
Comparison scores of six methods corresponding to Figs. 6 and 7

	Scores corresponding to Figs. 6(b)–(g)			Scores corresponding to Figs. 7(c)–(h)		
FCM_S1	0.6741	0.3975	0.9766	0.9958	0.7080	0.9253
FCM_S2	0.6600	0.3871	0.9789	0.9988	0.7068	0.9228
EnFCM	0.6753	0.3802	0.9698	0.9959	0.6963	0.9215
FGFCM_S1	0.6752	0.3802	0.9698	0.9940	0.6508	0.9110
FGFCM_S2	0.6396	0.3749	0.9802	0.9985	0.6868	0.9185
FGFCM	**0.7126**	**0.4382**	**0.9830**	**0.9988**	**0.7817**	**0.9437**

Concretely, $\xi-1, \xi-2, \xi-3$ and $\xi-4$ are generated on Fig. 8(a) according to Eq. (16) with respect to the four definitions of S_{ij} in Eqs. (18)–(20), and (12), respectively, and the corresponding parameters are $c=8$, $\alpha=0.8$ in Eq. (18) and $\lambda_g=1$ in Eq. (12), respectively.

Fig. 8(a) is a high-resolution T1-weighted phantom [32] (181×181 pixels) with slice thickness of 1 mm, 3% noise and no gray inhomogeneous as experimental object, the slice in the axial plane with the sequence of 91 and Fig. 8(b) is the after-filtered image $\xi-1$. We execute fast segmentation and FCM method on the image $\xi-1$ and the corresponding segmenting results are, respectively, displayed in Figs. 8(c) and (d) which are visually almost the same. The similar segmentation results can be obtained for the both segmentation

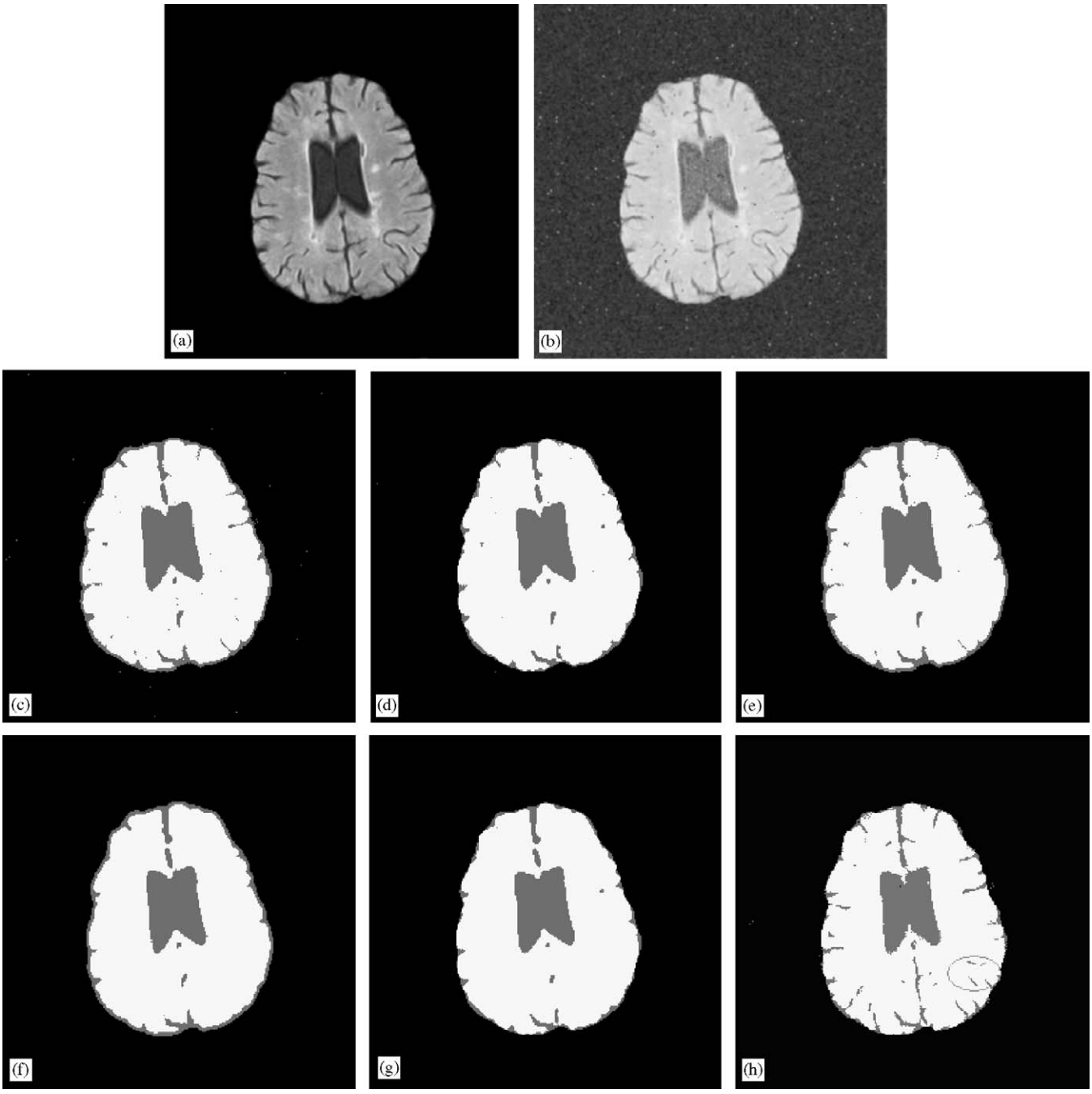

Fig. 7. Segmentation results obtained by using 5×5 local windows on a simulated brain MR image: (a) original brain MR image, (b) the same image with mixed noise, (c) using FCM_S1, (d) using FCM_S2, (e) using EnFCM, (f) using FGFCM_S1, (g) using FGFCM_S2, and (h) using FGFCM.

methods on the images $\xi-2$, $\xi-3$ and $\xi-4$, respectively, and thus we omit the segmenting images here.

Table 3 gives comparisons of iteration step, execution time and the number of different pixels of segmentation results between fast segmentation and FCM method for images $\xi-1$, $\xi-2$, $\xi-3$ and $\xi-4$. From Table 3, we can obviously see that the iteration step of fast segmentation is less than that of FCM, and the execution time (CPU: 2.66 GHz, Memory: 512 M, Operating system: windows XP, Software: Matlab 7.0) of fast segmentation is drastically reduced compared with FCM due to both the less iterations and only dependence on the number of the gray-levels q (256) rather than the image size itself N (181×181). We can also compute the segmentation difference in pixel after labeling each pixel of the image, respectively, using both algorithms and record their percentage of the differences accounting for the image. From the same table, we observe that the percentage is so small (below 1.3%) that it can almost be ignored, and

Table 3
Comparison between fast segmentation and FCM algorithms

Generated image	Iteration step		Running time (s)		Number of pixels different between fast segmentation and FCM	
	Fast segmentation	FCM	Fast segmentation	FCM		
$\xi-1$	223	277	0.24	37.58	305	0.93%
$\xi-2$	309	375	0.35	48.14	399	1.22%
$\xi-3$	118	137	0.13	18.61	0	0%
$\xi-4$	115	130	0.13	18.36	258	0.79%

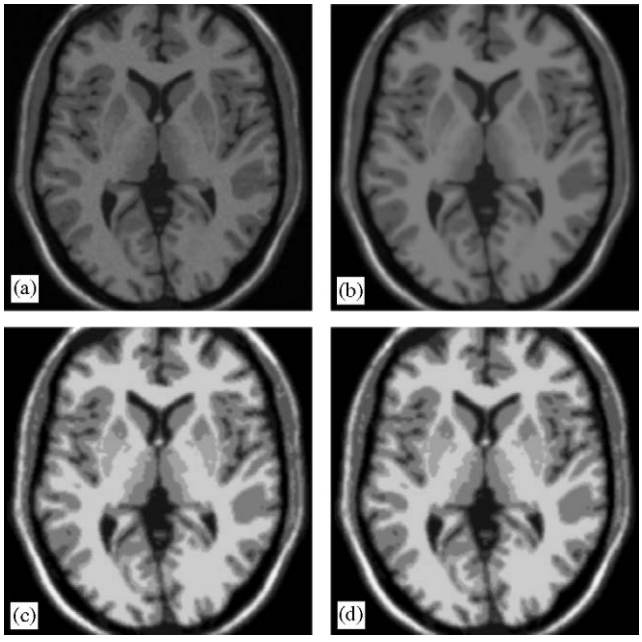

Fig. 8. Segmentation results on a simulated brain MR image: (a) original T1-weighted image, (b) the after-filtered image $\xi-1$, (c) using fast segmentation for $\xi-1$, and (d) using FCM for $\xi-1$.

therefore we can conclude that the segmenting performance of both fast segmentation and FCM applied on the same image are almost the same. On the whole, the fast segmentation can dramatically speed up FCM and obtain almost same segmentation results as FCM at the same time.

5. Conclusion

In this paper we presented a novel fast and robust FCM framework for image segmentation: fast generalized fuzzy c-means (FGFCM) clustering algorithms of incorporating local spatial and gray information. FGFCM introduces a new factor S_{ij} as a local (spatial and gray) similarity measure with aiming to guarantee both robustness to noise and detail-preserving for image, and at the same time remove the empirically-adjusted parameter α. On the other hand, FGFCM produces fast clustering for given image, which attributes to its dependence only on the number of the gray-levels q rather than the size N ($\gg q$, generally) of the image, consequently, its time complexity of clustering is reduced from $O(NcI_1)$ to $O(qcI_2)$. FGFCM can also be considered as a general framework and many other algorithms (Fast FCM, EnFCM, FGFCM_S1 and FGFCM_S2) can also be derived as its special cases for image segmentation.

The results reported in this paper show that our proposed algorithm is general, simple and appropriate for the images with various types of noises and the images with no noise. On the other hand, it is fast and thus suitable for large-sized gray images.

Fast clustering method used in FGFCM seems to be able to be straightforwardly extended to the segmenting algorithms for color images. However a problem will arise, i.e., the combination of the three color values achieves 2^{24} for a 24-bit RGB image, which is generally larger than the number of image pixels. Therefore, special preprocessing of the color image should be done before segmenting the given color image.

Within the framework of FGFCM, the mean-LogCauchy (MLC) filter [28] can be incorporated to promote the clustering performs in present of mixed noise. MLC, a convex combination of the mean and the LogCauchy filters, has experimentally been proven capable to achieve best performance in removing the mixed noise.

Our ongoing and further works include clustering validity in our algorithms, adaptive determination for the clustering number and other applications, e.g., gain field estimation.

Acknowledgments

The authors would like to thank the anonymous referees for their helpful comments and suggestions to improve the presentation of this paper. This work was supported by the National Science Foundation of China under Grant No. 60505004, Jiansu Postdoctoral Science Foundation and the Jiangsu Science Foundation under Grant No. BK2004001 and BK2006521.

References

[1] J.C. Bezdek, L.O. Hall, L.P. Clarke, Review of MR image segmentation techniques using pattern recognition, Med. Phys. 20 (1993) 1033–1048.

[2] D.L. Pham, C.Y. Xu, J.L. Prince, A survey of current methods in medical image segmentation, Annu. Rev. Biomed. Eng. 2 (2000) 315–337.
[3] W.M. Wells, W.E. LGrimson, R. Kikinis, S.R. Arrdrige, Adaptive segmentation of MRI data, IEEE Trans. Med. Imag. 15 (1996) 429–442.
[4] J.C. Bezdek, Pattern Recognition with Fuzzy Objective Function Algorithms, Plenum, New York, 1981.
[5] J.K. Udupa, S. Samarasekera, Fuzzy connectedness and object definition: theory, algorithm and applications in image segmentation, Graph. Models Image Process. 58 (3) (1996) 246–261.
[6] S.M. Yamany, A.A. Farag, S. Hsu, A fuzzy hyperspectral classifier for automatic target recognition (ATR) systems, Pattern Recognition Lett. 20 (1999) 1431–1438.
[7] M.S. Yang, Y.J. Hu Karen, C.R. Lin, C.C. Lin, Segmentation techniques for tissue differentiation in MRI of ophthalmology using fuzzy clustering algorithms, Magnetic Resonance Imaging 20 (2) (2002) 173–179.
[8] G.C. Karmakar, L.S. Dooley, A generic fuzzy rule based image segmentation algorithm, Pattern Recognition Lett. 23 (10) (2002) 1215–1227.
[9] D.L. Pham, J.L. Prince, An adaptive fuzzy *c*-means algorithm for image segmentation in the presence of intensity inhomogeneities, Pattern Recognition Lett. 20 (1999) 57–68.
[10] Y.A. Tolias, S.M. Panas, On applying spatial constraints in fuzzy image clustering using a fuzzy rule-based system, IEEE Signal Process. Lett. 5 (1998) 245–247.
[11] Y.A. Tolias, S.M. Panas, Image segmentation by a fuzzy clustering algorithm using adaptive spatially constrained membership functions, IEEE Trans. Systems Man Cybernet. A 28 (1998) 359–369.
[12] A.W.C. Liew, S.H. Leung, W.H. Lau, Fuzzy image clustering incorporating spatial continuity, Inst. Elec. Eng. Vis. Image Signal Process. 147 (2000) 185–192.
[13] D.L. Pham, Fuzzy clustering with spatial constraints, in: IEEE Proceedings of the International Conference Image Processing, New York, 2002, pp. II-65–II-68.
[14] M.N. Ahmed, S.M. Yamany, N. Mohamed, A.A. Farag, T. Moriarty, A modified fuzzy *c*-means algorithm for bias field estimation and segmentation of MRI data, IEEE Trans. Med. Imaging 21 (2002) 193–199.
[15] S.C. Chen, D.Q. Zhang, Robust image segmentation using FCM with spatial constraints based on new kernel-induced distance measure, IEEE Trans. Systems Man Cybernet. B 34 (4) (2004) 1907–1916.
[16] L. Szilágyi, Z. Benyó, S.M. Szilágyii, H.S. Adam, MR brain image segmentation using an enhanced fuzzy *c*-means algorithm, in: 25th Annual International Conference of IEEE EMBS, 2003, pp. 17–21.
[17] M.N. Ahmed, S.M. Yamany, N.A. Mohamed, A.A. Farag, T. Moriarty, Bias field estimation and adaptive segmentation of MRI data using modified fuzzy *c*-means algorithm, in: Proceedings of the IEEE International Conference on ComputerVision and Pattern Recognition, vol. 1, 1999, pp. 250–255.
[18] J. Leski, Toward a robust fuzzy clustering, Fuzzy Sets Systems 137 (2) (2003) 215–233.
[19] R.J. Hathaway, J.C. Bezdek, Generalized fuzzy *c*-means clustering strategies using *L* norm distance, IEEE Trans. Fuzzy Systems 8 (2000) 572–576.
[20] K. Jajuga, *L* norm based fuzzy clustering, Fuzzy Sets Systems 39 (1) (1991) 43–50.
[21] K.L. Wu, M.S. Yang, Alternative *c*-means clustering algorithms, Pattern Recognition 35 (2002) 2267–2278.
[22] K.R. Tan, S.C. Chen, Robust image denoising using kernel-induced measures, Proceedings of the 17th International Conference on Pattern Recognition, Cambridge, UK, 2004.
[23] P.J. Huber, Robust Statistics, Wiley, New York, 1981.
[24] X. He, P. Niyogi, Locality preserving projections, Advances in Neural Information Processing Systems, vol. 16, MIT Press, Cambridge, 2003.
[25] D.Q. Zhang, S.C. Chen, A novel kernelised fuzzy *c*-means algorithm with application in medical image segmentation, Artif. Intell. Med. 32 (1) (2004) 37–50.
[26] M.S. Yang, K.L. Wu, A similarity-based robust clustering method, IEEE Trans. Pattern Anal. Mach. Intell. 26 (4) (2004) 434–447.
[27] E.E. Kuruoglu. C. Molina, S.J. Gosdill, W.J. Fitzgerald, A new analytic representation of the α-stable density function, in: Proceedings of the American Statistical Society, 1997.
[28] A.B. Hamza, H. Krim, Image denoising: a nonlinear robust statistical approach, IEEE Trans. Signal Process. 49 (12) (2001) 3045–3053.
[29] Mathworks, Natick, MA, Image Processing Toolbox, [Online] Available:⟨http://www.mathworks.com⟩.
[30] C.T. Lin, C.S.G. Lee, Real-time supervised structure/parameter learning for fuzzy neural network, Proceedings of the 1992 IEEE International Conference on Fuzzy Systems, San Diego, CA, pp. 1283–1290.
[31] F. Masulli, A. Schenone, A fuzzy clustering based segmentation system as support to diagnosis in medical imaging, Artif. Intell. Med. 16 (2) (1999) 129–147.
[32] R.K.S. Kwan, A.C. Evans, G.B. Pike, An extensible MRI simulator for post-processing evaluation, Visualization in Biomedical Computing, Lecture Notes in Computer Science, vol. 1131, 1996, pp. 135–140.

About the Author—WEILING CAI received a B.Sc. from Nanjing University of Aeronautics & Astronautics (NUAA), PR China. Currently she is a Ph.D. Student at the Department of Computer Science & Engineering, NUAA. Her research interests focus on Neural Computing and Pattern Recognition.

About the Author—SONGCAN CHEN received the B.Sc. degree in Mathematics from Hangzhou University (now merged into Zhejiang University) in 1983. In December 1985, he completed the M.Sc. degree in Computer Applications at Shanghai Jiaotong University and then worked at Nanjing university of Aeronautics & Astronautics (NUAA) in January 1986 as an Assistant Lecturer. There he received a Ph.D. degree in Communication and Information Systems in 1997. Since 1998, as a full Professor, he has been with the Department of Computer Science and Engineering at NUAA. His research interests include pattern recognition, machine learning and neural computing. In these fields, he has authored or coauthored over 90 scientific journal papers.

About the Author—DAOQIANG ZHANG received the B.S. and Ph.D. degrees in Computer Science from Nanjing University of Aeronautics and Astronautics, China, in 1999 and 2004, respectively. He joined the Department of Computer Science and Engineering of Nanjing University of Aeronautics and Astronautics as a Lecturer in 2004, and is also a Postdoctoral Fellow of the LAMDA group at Nanjing University at present. His research interests include machine learning, pattern recognition, data mining, and image processing. In these areas he has published over 20 technical papers in refereed international journals or conference proceedings.